

Electrosynthesis of gold nanoparticles mediated by methylviologen using a gold anode in single compartment cell

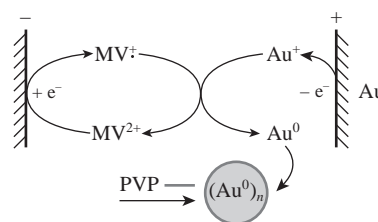
Vitaliy V. Yanilkin,^{*a} Natalya V. Nastapova,^a Gulnaz R. Nasretdinova^a and Yurii N. Osin^b

^a A. E. Arbutov Institute of Organic and Physical Chemistry, Kazan Scientific Centre, Russian Academy of Sciences, 420088 Kazan, Russian Federation. Fax: +7 843 275 2253; e-mail: yanilkin@iopc.ru

^b Interdisciplinary Center for Analytical Microscopy, Kazan (Volga Region) Federal University, 420018 Kazan, Russian Federation

DOI: 10.1016/j.mencom.2017.05.019

Methylviologen mediated reduction of Au^I ions generated *in situ* by dissolution of a gold anode in single compartment cell has been used for the electrosynthesis of spherical gold nanoparticles (Au-NPs) stabilized by poly(*N*-vinylpyrrolidone). The size of Au-NPs was from 15±6 to 27±9 nm, depending on the electrosynthesis conditions. Au-NPs were characterized by cyclic voltammetry, UV-VIS spectroscopy, dynamic light scattering, scanning and transmission electron microscopy.



The interest in metal nanoparticles (M-NPs) has been increasing lately due to their unique properties and diverse potential applications in catalysis, electronics, biomedicine, optics, analysis, etc.^{1–7} Currently, chemical reduction of metal ions and metal complexes in solution is the most thoroughly developed and popular method for their synthesis. For example, Au-NPs were prepared using a number of different reducing agents, in particular, hydrogen,⁸ sodium citrate, and ascorbic acid.⁹ Electroreduction of metal ions and metal complexes is widely used for M-NP preparation on an electrode surface¹⁰ and is rather rarely used for the electrosynthesis of M-NPs in bulk solution. Deposition of metals generated on the electrode surface is the main factor that restricts the use of electrochemistry. Therefore, in all developed methods for M-NP electrosynthesis in bulk solution the deposition problem has to be solved. In the pulse sonoelectrochemistry method,^{11–13} the formation of NPs on the electrode surface during short-time electroreduction is combined with their subsequent transfer to the solution by sonication of the electrode. In the method developed by Reetz *et al.*,^{14–18} the electroreduction of ions is performed in aprotic organic media using tetraalkylammonium or phosphonium salts as supporting electrolytes. For the same purpose, we have suggested the mediated electrosynthesis method,^{19–28} which differs from those mentioned above by moving the step of metal ion reduction from the electrode surface to the bulk solution. In this case, a mediator is reduced on the cathode, then reduced form of the mediator diffuses into the solution and reduces metal ion or metal complex. Thus, metal deposition on the electrode is minimized or completely avoided. The method applicability and efficiency were recently demonstrated by preparing Pd,^{19–21} Ag,^{22,23} Co,²⁴ Au,^{25–27} and Pt NPs.²⁸ The following compounds were used as the mediators: methylviologen (MV²⁺), either free or immobilized on the calix[4]-resorcin platform, anthracene, oxygen, and C₆₀ fullerene. Au-NPs were obtained by electroreduction of Au^I in two-compartment cell using MV²⁺, oxygen, and fullerene as the mediators.

In this paper, we report the electrosynthesis of Au-NPs stabilized with poly(*N*-vinylpyrrolidone) (PVP). The electro-

synthesis was performed by *in situ* generation of metal ions from the Au anode in aqueous media and by reduction with methylviologen in single compartment cell. It is known²⁹ that active anodic dissolution of gold in aqueous media occurs in the presence of chloride ions. Therefore, 0.1 M NaCl was used as supporting electrolyte.

The cyclic voltammetry (CV) curves of the gold electrode in this electrolyte exhibit active dissolution at 0.80–1.30 V vs. SCE and an electrode passivation at more positive potentials (Figure 1). The reverse CV curve demonstrates two re-reduction peaks C₁ and C₂ at 0.70 and 0.48 V, respectively. The C₁ peak is considerably weakly expressed, and C₂ is the main peak corresponding to the re-reduction of the generated gold ions. If the scanned potentials are limited to the active dissolution region, the shape of the reverse CV branch remains the same, but the C₂ peak is slightly (by 40 mV) shifted to less anodic potentials.

Reduction of Au^I (AuCl or [AuCl₂])²⁵ and HAuCl₄ occurs at similar potentials; the peak potentials on a glassy carbon (GC) electrode are 0.22 and 0.30 V, respectively (Figures S1 and S2, Online Supplementary Materials). Therefore, CV curves show that gold anode is dissolved, but do not provide information about the oxidation product. The nature of the C₁ peak also remains unclear.

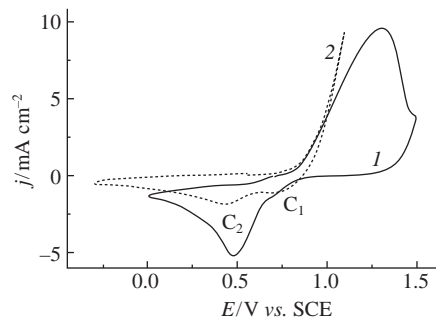


Figure 1 CV curves recorded on an Au electrode in aqueous 0.1 M NaCl solution in the potential region of (1) 1.5–0.0 V and (2) 1.1 to –0.3 V. $v = 100 \text{ mV s}^{-1}$.

Table 1 Conditions and results of methylviologen mediated and non-mediated single compartment cell electrolysis with the gold anode in H₂O/0.1 M NaCl medium.

Entry	Mediator	pH	PVP	Electrolysis parameters ^a				GC cathode		Au anode		
				Mode	<i>E</i> /V	<i>-I</i> /mA	<i>Q</i> /F	<i>S</i> /cm ²	Mass gain/mg	<i>S</i> /cm ²	Mass loss/mg	CE (%)
1	Methylviologen, 2 mM	5.0	Present	P	-0.85	~1.0	1.00	2.4	0.0	2.4	3.0	68
2		5.0	Present	G	-(0.99–0.86)	2.0	1.00	3.4	0.0	2.4	1.8	41
3		3.0	Present	P	-0.90	~2.0	1.00	3.0	0.0	2.4	2.0	46
4		3.0	Present	P	-0.80	1.22–1.49	1.00	3.0	0.0	2.4	1.4	32
5	No mediator	5.0	Absent	P	1.00	~1.0	0.10	3.0	0.0	2.1	0.4	100
6		5.0	Absent	P	1.00	1.00–0.42	0.75	3.0	1.3	2.1	1.5	71
7		5.0	Absent	G	0.95–1.00	1.0	1.00	3.0	0.8	2.1	1.5	50
8		3.0	Absent	P	1.00	~1.0	1.00	3.0	1.5	2.1	2.6	87
9		3.0	Present	P	1.00	~1.5	1.00	3.0	0.7	2.1	1.3	43

^aP is potentiostatic mode, G is galvanostatic mode; PVP concentration is 75 mM with respect to the monomeric unit; the amount of electricity *Q* was calculated assuming Au^I concentration equal to 1.5 mM, electrolyte volume in the presence of the mediator was 15 ml, or 10 ml without mediator; the stirring rate with a magnetic stirrer was 250 rpm in the electrolysis for entry 4, or 500 rpm in other cases; the temperature was 295 K.

The dissolution of gold to Au^{III} involves Au^I generation as the primary intermediate, which is not oxidized in the potential range of gold active dissolution (Figure S1). On this basis, we believe that Au^I is the product of the anodic dissolution of gold. Some difference in the potentials of the Au^I reduction peak on GC and the re-reduction peak on an Au electrode results from easier reduction of Au^I on the gold electrode due to nucleation of the generated Au⁰. All subsequent calculations relied on the assumption that dissolution of the gold electrode yields Au^I. The efficient electrosynthesis of Au-NPs performed previously^{25–27} was based exactly on the reduction of Au^I.

The CV curves of MV²⁺ recorded at pH 3.0 and 5.0 show two one-electron reduction peaks that are typical of this compound (*E*_{p1} = -0.70 V, *E*_{p2} = -1.05 V) (Figure S3), corresponding to the formation of a cation radical and a neutral diamine, respectively (Scheme S1). The first reduction peak to the cation radical is reversible at both pH values, and its parameters remain unchanged upon addition of PVP to the solution. However, the second reduction step is complicated by the adsorption of the resulting diamine, which is enhanced in the presence of PVP (pH 5.0), or by its fast irreversible chemical reactions (pH 3.0). Hence, under all studied conditions, MV²⁺ can serve as a mediator at potentials of the first reduction step to the cation radical.

Based on the voltammetric data obtained, the preparative single compartment cell electrolysis with gold anode was carried out in potentiostatic and galvanostatic modes at the controlled potential of the first mediator reduction step. In this case, the anodic current densities were always much lower than the current density maximum of gold anode dissolution, *i.e.*, the potential of the gold anode corresponded to its active dissolution region. The electrolysis results are presented in Tables 1 and 2.

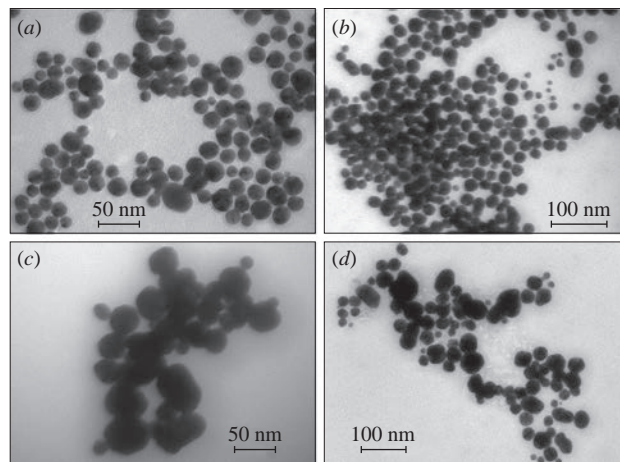
It is clear from Table 1 that the dissolution of the gold anode occurs in all cases (entries 1–4), however the current efficiency (CE) with respect to Au^I is much lower than the theoretical value. No noticeable amount of metal is deposited on the cathode in this case. The solution changes from colorless to crimson during all experiments. Moreover, at the start of the electrolysis, the solution layer in the proximity of cathode acquires the blue color of methylviologen radical cations (Figure S4). The CV curves of the solution after the electrolysis show methylviologen reduction peaks in the cathodic region with the original intensity. The Au^I reduction peak is either missing (entries 1, 2) or weak (entries 3, 4) (Figure S5). Hence, methylviologen is not consumed during the electrolysis and Au^I is not accumulated in the solution. Au-NP oxidation peak is recorded in the anodic potential region. Its height increases with the time of electrode exposure in the solution without stirring and without applying of the potential (Figure S6).

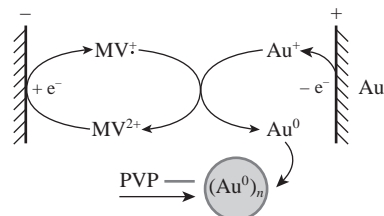
Table 2 Characteristics of PVP-stabilized Au-NPs obtained in electrolyses (entries 1–4, see Table 1).

Entry	<i>E</i> _A /V	<i>λ</i> /nm	Size/nm				C/Au ratio ^a
			DLS		Electron microscopy		
			by number	by intensity	SEM	TEM	
1	0.96	526	13	18, 107, 371, 5493	20±3	15±6	4.8
2	0.98	530	21, 53	24, 149, 679, 5122	23±5	19±5	4.8
3	0.99	532, 610	25	33, 155	30±8	27±9	0.6
4	1.00	535	18, 59	25, 164	30±8	26±9	1.4

^aAccording to the energy dispersive spectrum.

Apparently, the generated Au-NPs are adsorbed on the GC electrode and oxidized at potentials of gold anode dissolution. The presence of Au-NPs in the solution is also demonstrated by an absorption at 526–610 nm that is characteristic of these nanoparticles^{25–27} (Figure S7). According to TEM data, Au-NPs have spherical shape (Figure 2) and the sizes from 15±6 to 27±9 nm, depending on the electrolysis conditions (Table 2). The latter also affect the ratio of the metal core and stabilizing PVP shell, as indicated by the differences in the carbon/gold ratio according to the data of energy dispersive analysis (Table 2, Figure 3, Figure S8). Presumably, it means that the thickness of the PVP shell weakly depends on the Au-NP size. SEM (Figure S9)

**Figure 2** TEM images of Au-NPs obtained in electrolyses (see Table 1): (a) entry 1, (b) entry 2, (c) entry 3 and (d) entry 4.



Scheme 1 Methylviologen mediated electro-synthesis of Au-NPs using a soluble Au anode.

can be used to determine the sizes of Au-NPs, including the PVP shell (Au-NP@PVP), isolated and deposited on a titanium support. DLS method (Figure S10) can be used to determine the mean hydrodynamic diameter of Au-NPs with PVP and hydrate shells in the solution [(Au-NP@PVP)_{hydr}]. The Au-NP size affects the absorption band wavelength and the oxidation potential. Therefore, in general, a correspondence between various characteristics of the Au-NPs obtained in our experiments is observed (Table 2). The lower the PVP: Au ratio, the larger the Au-NP; the closer the minimum size of NPs obtained by DLS and SEM methods to the sizes obtained by TEM, and the higher the wavelength λ and the oxidation peak potential E_A . It should be noted that DLS and SEM methods also detect much larger particles. Probably these are NP aggregates formed due to agglomeration of PVP shells.

Thus, spherical PVP-stabilized Au-NPs with various sizes can be obtained by varying the conditions of electrolysis in methylviologen mediated reduction of Au^I ions generated *in situ* by dissolution of the gold anode (Scheme 1). The reduction at pH 5.0 occurs almost quantitatively, but dissolution of the metal occurs inefficiently. Two reasons may be responsible for this, *viz.*, reoxidation of the Au-NPs on the gold anode and side oxidation of solution components. To clarify the reason, we performed a series of similar experiments in the absence of mediator. We assumed that in this case, the metal being generated would mainly be deposited on the cathode, since reduction of Au^I would occur there. Hence, the oxidation of Au-NPs would be excluded or minimized.

In the absence of mediator, gold anode is dissolved in all electrolyses almost as inefficiently, but a fraction of electricity (32–68%) is consumed for metal dissolution, while remaining commensurable fraction is consumed in a side process (see Table 1). Moreover, the CE decreases with time. In all cases, both in the absence and even in the presence of PVP, about half of the dissolved metal is deposited on the cathode, as follows from the formation of a gold deposit on the cathode (Figure S11) and the mass gain of the latter (Table 1). The other fraction remains in the solution in the form of Au^I, as indicated by the presence of Au^I peak on the CV curves of the solution after the electrolysis (Figure S12). Most likely, prolonged electrolysis results in gradual passivation of the gold electrode. While metal dissolution predominates at the beginning of electrolysis, this process is ‘blocked’ with time and side oxidation process starts to prevail. It can be assumed as a hypothesis that upon anodic polarization, along with gold dissolution, competitive oxidation of chloride ions to molecular chlorine occurs, and the C₁ peak on the CV curves (Figure 1) is due to the reduction of the latter. Chlorine, as a strong oxidant, quickly oxidizes methylviologen radical cations to the original state, so it is not accumulated in the solution and methylviologen is not consumed.

In conclusion, the results on non-mediated electrolysis demonstrate that the main reason of inefficient gold oxidation in mediated electro-synthesis of Au-NPs lies not in the oxidation of generated Au-NPs but in the side oxidation of solution components.

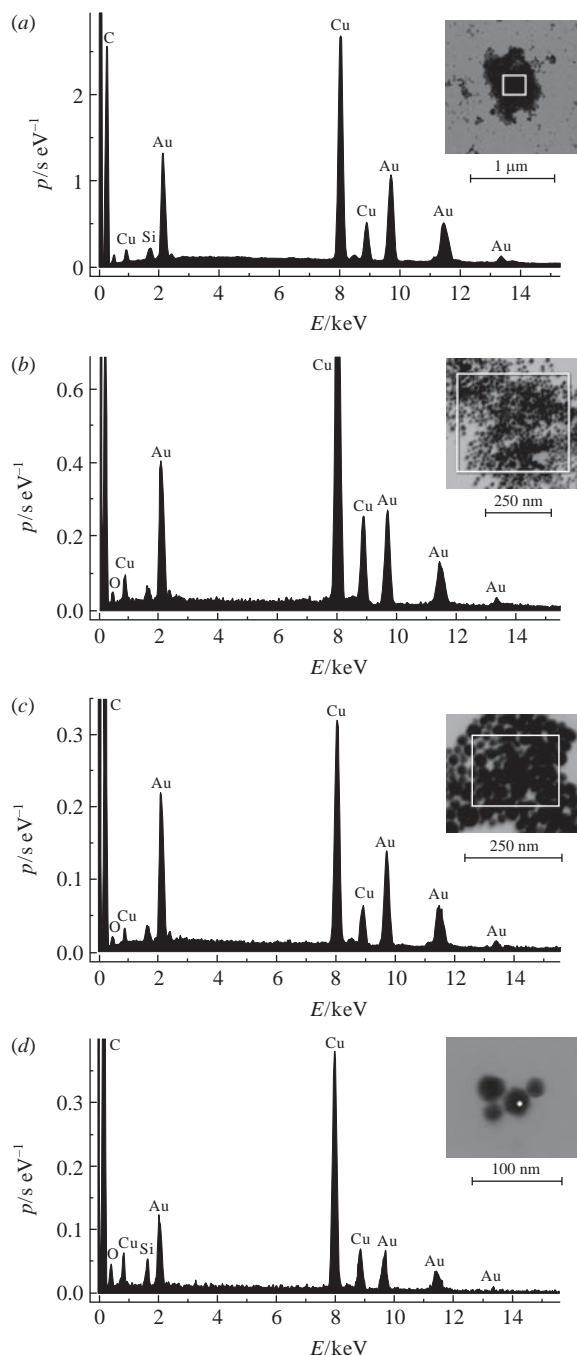


Figure 3 Energy-dispersive spectra of Au-PVP nanoparticles synthesized in electrolyses using a soluble Au anode (see Table 1): (a) entry 1, (b) entry 2, (c) entry 3 and (d) entry 4.

This study was supported by the Russian Science Foundation (project no. 14-23-00016).

Online Supplementary Materials

Supplementary data associated with this article can be found in the online version at doi: 10.1016/j.mencom.2017.05.019.

References

- 1 A. D. Pomogailo, A. S. Rosenberg and I. E. Uflyand, *Nanochastitsy metallov v polimerakh (Nanoparticles of Metals in Polymers)*, Khimiya, Moscow, 2002 (in Russian).
- 2 V. I. Roldughin, *Russ. Chem. Rev.*, 2000, **69**, 821 (*Usp. Khim.*, 2000, **69**, 899).
- 3 M. C. Daniel and D. Astruc, *Chem. Rev.*, 2004, **104**, 293.
- 4 I. P. Suzdalev, *Nanotehnologiya. Fiziko-khimiya nanoklasteroi, nanostruktur i nanomaterialov (Nanotechnology. Physical Chemistry of*

- Nanoclusters, Nanostructures and Nanomaterials*), KomKniga, Moscow, 2006 (in Russian).
- 5 V. V. Volkov, T. A. Kravchenko and V. I. Roldughin, *Russ. Chem. Rev.*, 2013, **82**, 465.
 - 6 L. A. Dykman, V. A. Bogatyrev, S. Yu. Shchegolev and N. G. Khlebtsov, *Zolotyie nanochastitsy. Sintez, svoystva, i biomeditsinskoe primeneniye (Gold Nanoparticles. Synthesis, Properties and Biomedical Applications)*, Nauka, Moscow, 2008 (in Russian).
 - 7 B. I. Kharisov, O. V. Kharissova and U. Ortiz-Mendez, *Handbook of Less-Common Nanostructures*, CRC Press, Boca Raton, 2012.
 - 8 G. N. Bondarenko and I. P. Beletskaya, *Mendeleev Commun.*, 2015, **25**, 443.
 - 9 M. S. Kotelev, D. S. Kopitsyn, I. A. Tiunov, V. A. Vinokurov and A. A. Novikov, *Mendeleev Commun.*, 2015, **25**, 356.
 - 10 O. A. Petrii, *Russ. Chem. Rev.*, 2015, **84**, 159.
 - 11 V. Sáez and T. J. Mason, *Molecules*, 2009, **14**, 4284.
 - 12 J. Zhu, S. Liu, O. Palchik, Y. Kolytyn and A. Gedanken, *Langmuir*, 2000, **16**, 6396.
 - 13 J. Reisse, T. Caulier, C. Deckerkheer, O. Fabre, J. Vandercammen, J. L. Delplancke and R. Winand, *Ultrason. Sonochem.*, 1996, **3**, 147.
 - 14 M. T. Reetz and W. Helbig, *J. Am. Chem. Soc.*, 1994, **116**, 7401.
 - 15 J. A. Becker, R. Schäfer, R. Festag, W. Ruland, J. H. Wendorff, J. Pebler, S. A. Quaiser, W. Helbig and M. T. Reetz, *J. Chem. Phys.*, 1995, **103**, 2520.
 - 16 M. T. Reetz, S. A. Quaiser and C. Merk, *Chem. Ber.*, 1996, **129**, 741.
 - 17 M. T. Reetz, W. Helbig, S. A. Quaiser, U. Stimming, N. Breuer and R. Vogel, *Science*, 1995, **267**, 367.
 - 18 M. T. Reetz, M. Winter, R. Breinbauer, T. Thurn-Albrecht and W. Vogel, *Chem. Eur. J.*, 2001, **7**, 1084.
 - 19 V. V. Yanilkin, G. R. Nasybullina, A. Yu. Ziganshina, I. R. Nizamiev, M. K. Kadirov, D. E. Korshin and A. I. Konovalov, *Mendeleev Commun.*, 2014, **24**, 108.
 - 20 S. Fedorenko, M. Jilkin, N. Nastapova, V. Yanilkin, O. Bochkova, V. Buriliov, I. Nizameev, G. Nasretdinova, M. Kadirov, A. Mustafina and Y. Budnikova, *Colloids Surf., A*, 2015, **486**, 185.
 - 21 G. R. Nasretdinova, Y. N. Osin, A. T. Gubaidullin and V. V. Yanilkin, *J. Electrochem. Soc.*, 2016, **163**, G99.
 - 22 G. R. Nasretdinova, R. R. Fazleeva, R. K. Mukhitova, I. R. Nizameev, M. K. Kadirov, A. Y. Ziganshina and V. V. Yanilkin, *Electrochem. Commun.*, 2015, **50**, 69.
 - 23 V. V. Yanilkin, N. V. Nastapova, G. R. Nasretdinova, R. R. Fazleeva, A. V. Toropchina and Yu. N. Osin, *Electrochem. Commun.*, 2015, **59**, 60.
 - 24 V. V. Yanilkin, G. R. Nasretdinova, Yu. N. Osin and V. V. Salnikov, *Electrochim. Acta*, 2015, **168**, 82.
 - 25 V. V. Yanilkin, N. V. Nastapova, G. R. Nasretdinova, S. V. Fedorenko, M. E. Jilkin, A. R. Mustafina, A. T. Gubaidullin and Yu. N. Osin, *RSC Adv.*, 2016, **6**, 1851.
 - 26 V. V. Yanilkin, N. V. Nastapova, G. R. Nasretdinova, R. R. Fazleeva and Yu. N. Osin, *Electrochem. Commun.*, 2016, **69**, 36.
 - 27 V. V. Yanilkin, N. V. Nastapova, G. R. Nasretdinova, Yu. N. Osin and A. T. Gubaidullin, *ECS J. Solid State Sci. Technol.*, 2017, **6**, M19.
 - 28 V. V. Yanilkin, N. V. Nastapova, G. R. Nasretdinova, R. R. Fazleeva, S. V. Fedorenko, A. R. Mustafina and Yu. N. Osin, *Russ. J. Electrochem.*, 2017, **53**, DOI: 10.7868/S0424857017050176 (*Elektrokhimiya*, 2017, **53**, 578).
 - 29 *Spravochnik po elektrokhimii (Handbook of Electrochemistry)*, ed. A. M. Suhotin, Khimiya, Leningrad, 1981 (in Russian).

Received: 12th October 2016; Com. 16/5070